Articles in PresS. Am J Physiol Lung Cell Mol Physiol (May 4, 2017). doi:10.1152/ajplung.00453.2016

REDUCED CARBOXYLESTERASE 1 IS ASSOCIATED WITH ENDOTHELIAL INJURY IN METHAMPHETAMINE INDUCED PULMONARY ARTERIAL HYPERTENSION

Mark E. Orcholski[1,2,3], Artyom Khurshudyan[4], Elya A. Shamskhou[1,2,3], Ke Yuan[1,2,3], Ian Y. Chen[3], Sean D. Kodani[5], Christophe Morisseau[5], Bruce D. Hammock[5], Ellen M. Hong[1,2,3], Ludmila Alexandrova[6], Tero-Pekka Alastalo[7], Gerald Berry[8], Roham T. Zamanian*[1,2,3] and Vinicio de Jesus Perez*[1,2,3]

*These authors contributed equally to this work.

[1]Division of Pulmonary and Critical Care Medicine, [2]The Vera Moulton Wall Center for Pulmonary Vascular Medicine and [3]Stanford Cardiovascular Institute, Stanford University Medical Center, Stanford, California. [4]University of Illinois College of Medicine, [5]Department of Entomology and Nematology, UC Davis Comprehensive Cancer Center, University of California Davis, Davis, California. [6]The Vincent Coates Foundation Mass Spectrometry Laboratory, Stanford University Mass Spectrometry, Stanford, California. [7]Children's Hospital Helsinki, University of Helsinki, Finland. [8]Department of Pathology, Stanford University Medical Center, Stanford, CA.

Corresponding Author: Vinicio A. de Jesus Perez, MD

Assistant Professor of Medicine

Division of Pulmonary and Critical Care Medicine

Stanford University Medical Center

300 Pasteur Drive, Grant S140b

Stanford, CA 94305

Email: vdejesus@stanford.edu

Phone: 1-650-723-0318

ABSTRACT

Pulmonary arterial hypertension is a complication of methamphetamine use (METH-PAH) but the pathogenic mechanisms are unknown. Given that cytochrome P450 2D6 (CYP2D6) and carboxylesterase 1 (CES1) are involved in metabolism of METH and other amphetamine-like compounds, we postulated that loss of function variants could contribute to METH-PAH. While no difference in CYP2D6 expression was seen by lung immunofluorescence, CES1 expression was significantly reduced in endothelium of METH-PAH microvessels. Mass spectrometry analysis showed that healthy pulmonary microvascular endothelial cells (PMVECs) have the capacity to both internalize and metabolize METH. Furthermore, whole exome sequencing data from 18 METH-PAH patients revealed that 94.4% of METH-PAH patients were heterozygous carriers of a single nucleotide variant (SNV, rs115629050) predicted to reduce CES1 activity. PMVECs transfected with this CES1 variant demonstrated significantly higher rates of METH-induced apoptosis. METH exposure results in increased formation of reactive oxygen species (ROS) and a compensatory autophagy response. Compared to healthy cells, CES1-deficient PMVECs lack a robust autophagy response despite higher ROS, which correlates with increased apoptosis. We propose that reduced CES1 expression/activity could promote development of METH-PAH by increasing PMVEC apoptosis and small vessel loss.

Words: 185 (200 Max)

INTRODUCTION

Pulmonary Arterial Hypertension (PAH) is a life-threatening disease characterized by abnormally elevated pulmonary pressure and right heart failure with a median survival of 3 years after diagnosis (20). Lung pathology in PAH patients is characterized by marked loss of distal pulmonary microvessels and severe obliterative vasculopathy, which progressively overwhelms the capacity of the right heart to pump venous blood into the lungs (43). Current treatments include vasodilatory drugs that help palliate symptoms but fail to prevent disease progression, leaving lung transplantation as the only therapy for patients with end-stage PAH (18).

Available evidence supports a key role for interaction between genes and environment in triggering PAH in susceptible individuals. This is the case for PAH associated with exposure to certain drugs and toxins, where patients develop a clinical and pathological picture that is indistinguishable to other forms of PAH (1, 5, 47). The 2015 ESC/ERS guidelines now recognize 16 different compounds associated with PAH, which range from FDA approved therapies (e.g. mitomycin, dasatanib) to illicit stimulants such as methamphetamine (METH) (19). Methamphetamine is a highly addictive compound whose popularity among young and middle age adults has steadily increased worldwide in the past decade. In addition to being a potent neurostimulant, METH can also affect other organs such as the kidneys, brain and liver, resulting in severe organ dysfunction and premature death (21). While METH use is associated with a higher incidence of

cardiovascular disease such as ischemic cardiomyopathy, arrhythmias and myocardial infarction, it is only recently that PAH has been recognized as a life-threatening complication of METH use. The association between inhaled METH use and PAH was first reported by Schaiberger *et al.* and further supported by a retrospective study by Chin *et al.* that found significantly higher rates of METH use in patients diagnosed with idiopathic PAH (IPAH) when compared to other PAH groups (10, 51). PET studies have shown that [(11)C] d-METH administered intravenously localizes primarily in the lung tissue, suggesting that the lung is a primary target for METH related injury (58). On the basis of these studies, METH use was included in the most recent clinical classification of pulmonary hypertension as a likely risk factor in drug and toxin induced PAH (D+T PAH) (20).

While the true incidence and prevalence of METH-PAH in the US is unknown, we have seen a disturbing increase in the number of METH-PAH cases diagnosed at the Stanford Adult Pulmonary Hypertension Clinic over the last ten years. At present, 85% of our D+T PAH patients carry a diagnosis of METH-PAH and their median 5-year survival is estimated at 35% (R. Zamanian, personal communication), which is significantly worse compared to that of IPAH patients. Despite the current clinical evidence, it must be emphasized that not all patients with a history of METH use develop PAH. Similar to patients with familial and sporadic PAH, it is possible that variations in certain genes may be required to trigger PAH in a subset of METH users but no gene candidates have been established in any study to date.

Two major liver enzyme families carry out metabolism of most amphetamine derivatives: the cytochrome P450 2D6 (CYP2D6) and carboxylesterase 1 (CES1). CYP2D6 is an isoenzyme belonging to the cytochrome P450 family required for phase 1 metabolism of a wide range of drugs. CES1 is a key enzyme in the detoxification of illicit toxins such as cocaine and heroin as well as FDA approved drugs such as methylphenidate (Ritalin), an amphetamine-derived drug used in the treatment of attention deficit disorders (28, 62). Polymorphisms that reduce expression and/or activity of either enzyme can affect the rate of drug metabolism and result in chronic organ injury (6, 13, 39, 55, 65) (32), but whether this could also be linked to METH induced pulmonary vascular injury is unknown. On the basis of these findings, we speculated that loss of function of CYP2D6 and/or CES1 could increase risk of PAH in METH users. Here, we present for the first time evidence that pulmonary endothelial cells can metabolize METH and have identified CES1 as a candidate gene required for protecting the pulmonary endothelium against METH-related injury.

METHODS

Lung Tissue and Cell Culture

Lung tissue from healthy donors and METH-PAH patients was obtained via the Cardiovascular Medical Education and Research Fund–Pulmonary Hypertension Breakthrough Initiative (CMREF-PHBI). Healthy donor PMVECs were obtained from the CMREF-PHBI and a commercial source (Promocell, Germany, cat# C-12282). All cells were grown in EC media (ScienCell, Carlsbad, CA, cat# 1001) with growth supplements and used between passages 4-8. Methamphetamine was purchased from Sigma-Aldrich (St. Louis, MO, cat# M8750). A METH concentration of 5mM was chosen after conducting dose response studies on healthy PMVECs. To control for the different growth rates of PMVECs between experimental groups (siCES1/siCYP2D6 vs. siControl) cells were seeded into culture plates two hours before METH exposure in all *in vitro* experiments.

Immunofluorescence

Lung tissue from healthy donors, METH-PAH, IPAH, cystic fibrosis (CF), and idiopathic pulmonary fibrosis (IPF) patients were obtained from explanted lungs at the time of transplant or during autopsy and embedded in paraffin blocks or OCT. Paraffin-embedded

tissue sections were treated with xylene followed by serial dilutions of ethanol. The sections were then put into a beaker of boiling citrate buffer for 10 minutes. After the sections had cooled to room temperature, they were washed in PBS buffer. The slides were then incubated with diluted normal goat blocking serum, followed by incubation overnight with anti-CES1 (a kind gift of Dr. Bruce Hammock as described (67)), CD31 (LSBio, Seattle, WA, cat# B4737), or anti-CYP2D6 (Abcam, Boston, MA cat# 185625) primary antibody in a humidity chamber at 4^0C. The following day, the sections were washed three times for 5 minutes each in PBS then incubated for 1 hour with Alexa Fluor 488/594 conjugated secondary antibody (Thermo-Fisher, Waltham, WA. Following treatment with antifade reagent with DAPI (Cell Signaling, Danvers, MA, cat# 8961S), the slides were mounted and sealed.

Liquid Chromatography-Mass Spectrometry (LC-MS)

A unified LC-UV-MS method was used for structural elucidation of methamphetamine metabolites, using an 1100 series HPLC-UV (Agilent Technologies) integrated with an LTQ XL ion trap mass spectrometer (Thermo Fisher Scientific). Extraction procedure: 300 µL ice cold methanol was added to 100µl cell suspension. Solutions were sonicated, centrifuged, and the supernatant was removed and evaporated to dryness under nitrogen. The extract was reconstituted in 100µL of water, and 10µl was injected onto the HPLC column. Liquid chromatography (LC): Chromatography was performed on a 250 x 2.1 mm Polaris 5 C18-A column (Varian), using 0.1% formic acid in acetonitrile (B) and 0.1% formic acid in water (A) and eluting with a linear gradient from 0% B to 50% B in 25 minutes followed by increase to 95% B in 7 minutes. Total run time was 37 minutes. Flow

rate was 250 μL/min and UV detection was at 214 nm. Mass Spectrometry: MS^2 data for structural elucidation were acquired using heated electrospray ionization with positive/negative ion switching using full scan acquisition (110 – 600 m/z mass range) and data dependent acquisition in dynamic exclusion mode. Collision induced dissociation (CID) channel was set up for monitoring hydroxymethamphetamine metabolites (m/z=166.2 Da; isolation width 2 m/z).

Patient Selection and DNA Extraction

Written informed consent for this study was obtained in agreement with protocols approved by the institutional review boards (IRB# 5443) at Stanford University. METH-PAH was defined as PAH with no identifiable cause with a mean pulmonary arterial pressure (mPAP) greater than or equal to 25 mm Hg at rest, pulmonary artery wedge pressure (PAWP) less than or equal to 15 mm Hg and a pulmonary vascular resistance (PVR) greater than 3 Wood Units (WU)(2). Significant METH exposure was considered if the patient reported greater than a 3-month history of weekly METH use and reported no use of other stimulants associated with PAH. Genomic DNA was purified from buffy coat samples obtained from whole blood using the Ficoll extraction method and the Qiagen DNeasy kit following the manufacturer's protocol.

Whole Exome Sequencing

WES samples were prepared as an Illumina sequencing library, and in the second step, the sequencing libraries were enriched for the desired target using the Illumina Exome

Enrichment protocol. The captured libraries were sequenced in an Illumina HiSeq 2000 Sequencer (Illumina Inc., San Diego, CA) using paired-end 75- to 100-bp sequences. Samples were sequenced to at least 125-fold (3125) sequence coverage. Raw sequence reads were aligned to human reference sequence hg19 using SAM/BAM. Sequencing data were analyzed using ANNOVAR software (openbioinformatics.org). A list of CYP2D6 and CES1 candidate variants was prepared by selecting variants predicted to result in nonsynonymous protein-coding changes (missense, nonsense) and confirmed using Sanger sequencing. Given that all METH-PAH patients were Caucasians, we used the minor allele frequency (MAF) for European (non Finnish) whites reported in the latest version of the ExAC browser.

Allelic Discrimination qPCR

Genomic DNA was isolated from patient lung tissue embedded in paraffin using the QIAmp DNA FFPE Tissue Kit from Qiagen (Qiagen, Valencia, CA, Cat# 56404). First, three 10 μm sections were cut from paraffin block using a microtome then placed in 1 ml xylene, then DNA extraction was achieved by following the manufacture's instructions. Real-time PCR for CES1 SNP rs115629050 was performed using Taqman assays (Applied Biosystems, Foster City, CA, Cat# 4331349, Assay ID# AHMSYGO) on an ABI7500 PCR machine. Each reaction contains 11.25 μL isolated gDNA (~20ng), 12.5 μL PCR master mix (2x) and 1.25 μL TaqMan SNP probe (20x). The PCR reaction is 50 cycles of: step one 92^{o}C for 15 seconds and step two 60^{o}C for 1 minute, with an initial step of 95°C for 10 minutes. The StepOne Plus software generated the Allelic Discrimination Plot with the 2-Cluster Calling enabled.

209

210 **CES1 Activity Assay**

211 CES1 activity in peripheral blood mononuclear cells (PBMCs) was performed using the
212 CES1 Specific Activity Assay Kit (Abcam, Boston, MA, cat#109717) following the
213 manufacturer's protocol. Briefly, cells were pelleted and lysed with RIPA buffer. After
214 measuring protein concentration using the BCA protein assay (Thermo-Fisher, Waltham,
215 WA), samples were loaded on a 96 well plate coated with an antibody against CES1 and
216 incubated for 3 hours at room temperature with gentle shaking. After washing, CES1
217 enzyme activity was measured by adding 200□l of a 1 mM 4-nitrophenol (4-NP) solution
218 was loaded into each well followed by measurement of absorbance at 402nm at 15 minutes
219 using a Promega spectrophotometer. CES1 quantity per well was measured by incubating
220 with an anti-CES1 HRP tagged antibody for one hour followed by addition of DAB and
221 measurement of absorbance at 600nm via spectrophotometer. Results are expressed as
222 CES1 activity relative to quantity.

223

224 **Western Immunobloting**

225 PMVECs were washed twice with ice-cold 1 × PBS, and lysates were prepared by adding
226 lysis buffer (1XRIPA and 1mM PMSF), scraping into a 1.5-ml microcentrifuge tube, and
227 vortex homogenized before centrifugation. Supernatants were transferred to fresh
228 microcentrifuge tubes and stored at -80° C. The protein concentration was determined by
229 the BCA assay (Thermo-Fisher, Waltham, WA). Equal amounts of protein were loaded onto
230 each lane of a 4 – 12% Bis-Tris gel and subjected to electrophoresis under reducing
231 conditions. After blotting, PVDF membranes were blocked for 1 h (5% milk powder in 0.1%

PBS/Tween) and incubated with primary antibodies overnight at 4 °C. Bands were visualized using ECL (Thermo-Fisher, Waltham, WA) and loading was assessed with α-tubulin (Sigma-Aldrich, St. Louis, MO). Some western blot images show only the relevant lanes while those not associated with the current study have been removed. However, all grouped samples were run on the same gel.

CES1 and CYP2D6 siRNA Transfection

To achieve gene knockdown, 2μM siRNA against CES1 (GE Dharmacon cat# L-009051-00), CYP2D6 (ThermoFisher siRNA ID# s3834), or non-targeting siRNA control (GE Dharmacon cat# D-001810-10-05) were transfected into healthy PMVECs (Promocell, Germany, cat# C-12282). Knockdown efficiency of CES1 and CYP2D6 were evaluated 72 hours after nucleofection by measuring protein levels in cell lysates via Western blot. Transfection was performed using a Nucleofector 2b Device (program T-23) with the Basic Endothelial Cell Nucleofection kit (Lonza, Switzerland, cat# VPI-1001). All experiments were performed 72 hours after nucleofection.

Caspase 3/7 Apoptosis Assay

50μl of Caspase Glo-3/7 (Promega Cat# G8091) was added into each sample at a 1:1 ratio with culture medium and incubated in dark for 1 hour. The luminescence of each sample was measured in a plate reader Promega GloMAx luminometer (Promega, Madison, WI, Cat# E9032) following the manufacturer's protocol and normalized to media+Glo-3/7 without cells.

CES1 plasmids and transfection methods

Plasmids encoding the full length CES1 and control blank were purchased from OriGene (Rockville, MD) and a mutant construct containing the CES1 rs115629050 SNV was generated using in situ mutagenesis (Mutagenex, Suwanee, GA). Transfection of plasmids was performed using a Nucleofector 2b Device (program T-23) with the Basic Endothelial Cell Nucleofection kit. All experiments were performed 24 hours after nucleofection.

CellROX Assay for Reactive Oxygen Species

PMVECs were plated at 1.0 x 10^4 cells per well on eight-well EZ chamber slides (Millipore, Germany) and cultured overnight. Four hours after addition of METH, the cells were rinsed with 1X PBS once and treated with 5 μM CellROX® Green Reagent (Thermo-Fisher, Waltham, WA, cat# C10444) for 30 minutes at 37^{o}C. After incubation, cells were imaged live on a Leica DMRMII inverted microscope.

Autophagy Flux Analysis

Autophagy flux was assessed by Western blot analysis of P62 (Novus, Littleton, CO, cat# H00008878-M01) and LC3-II (Cell Signaling, Danvers, MA, cat# 12741) levels in the absence and presence of lysosomal blockade, which was specifically accomplished by incubating cells with 100 nM bafilomycin A1 (Sigma-Aldrich) for 2 hours as previously described (26).

Statistical analysis

The number of samples studied per experiment is indicated in the Figure Legends. Values from multiple experiments are expressed as mean±SEM. Statistical significance was determined using unpaired t-test or ordinary one-way ANOVA with Tukey's multiple comparison tests unless stated otherwise. A value of $P<0.05$ was considered significant.

RESULTS

CES1 exhibits differential expression in pulmonary microvessels of METH-PAH patients.

While CES1 and CYP2D6 expression is highest in the liver, BioGPS microarray and Illumina Human BodyMap RNA-seq atlas have shown that mRNA for these two enzymes is also expressed in lung and circulating peripheral blood mononuclear cells (PBMCs) (25, 31). To assess CES1 and CYP2D6 protein expression in pulmonary arteries, we performed immunofluorescence (IF) in lung tissue sections from two healthy donors and four METH-PAH patients obtained at the time of autopsy or transplant. Our studies demonstrated that CYP2D6 is expressed in the endothelium of small microvessels;

however, we found no difference in CYP2D6 expression between healthy donor and METH-PAH lungs (**Fig 1A).** In contrast, CES1 expression was found to be reduced or absent in remodeled vessels of all four METH-PAH samples as compared to healthy patient samples (**Fig. 1B**).

To determine whether our findings were specific to METH-PAH, we also performed IF on lung tissue from patients with IPAH, cystic fibrosis (CF) and idiopathic pulmonary fibrosis (IPF). Again, no difference in CYP2D6 expression was found in IPAH (**Fig. 2A**) or in CF and IPF lungs (**Fig 2B, C**). In contrast, we found that CES1 expression was substantially reduced in IPAH vascular lesions (**Fig. 2D**) but not in CF and IPF (**Fig. 2E, F**). Our observation of reduced CES1 expression in IPAH lungs is in agreement with the recent description of reduced CES1 expression in endothelial cells derived from IPAH inducible pluripotent stem cells (49).

Taken together, these studies demonstrate that both CES1 and CYP2D6 are expressed in pulmonary vessels but only the former appears to be differentially expressed in lungs of healthy and METH-PAH patients. As the next step, we sought to determine whether pulmonary microvascular endothelial cells (PMVECs) have the capacity to metabolize METH *in vitro*.

PMVECs can internalize and metabolize METH

Some cells can metabolize METH into the major metabolites amphetamine and p-hydroxymethamphetamine (p-OHMA) (**Fig 3A**), as well as other minor metabolites

(norephedrine, phenylacetone, benzoic acid and hippuric acid) and their intracellular accumulation may account for the toxicity of the parent compound (9, 53). To assess whether healthy human PMVECs have the capacity to metabolize METH, we analyzed cell media and lysates of METH treated PMVECs for metabolites using LC/MS. Analysis of cell media did not identify significant amounts of METH or any known metabolites in either the treated or non-treated group (data not shown), suggesting internalization and/or degradation of METH. However, analysis of cell lysates from METH treated PMVECs demonstrated at least six hydroxyl isomers of METH, likely including p-OHMA (**Fig. 3B**). Of note, no evidence of amphetamine was found.

While production of p-OHMA by PMVECs is likely driven by CYP2D6, the enzyme responsible for metabolizing METH in the liver (33), the role of CES1 in METH metabolism is unclear. It is important to point out that CES1 is an esterase known to break ester bonds in molecules; since METH does not have any ester bonds, it is unlikely to serve as a substrate for CES1. However, since CES1 was significantly reduced in METH-PAH, we sought to determine whether CES1 knockdown could affect METH metabolism in PMVECs. We reduced CES1 protein levels via siRNA transfection and exposed PMVECs treated with either control (siCt) or CES1 (siCES1) siRNA to METH for four hours followed by LC/MS. We found no difference in the METH metabolite profile of CES1 siRNA treated PMVECs compared to nontransfected or siCt transfected cells (data not shown).

It is important to note that our LC/MS only looked at direct METH metabolites (phase I reaction) and did not capture information regarding other metabolites (e.g. toxic esters)

generated in cells when exposed to METH (36). Thus, while CES1 is not involved in phase 1 metabolism of METH, it could be required to neutralize toxic metabolites produced by METH metabolism.

METH-PAH patients demonstrate high prevalence of a potentially pathogenic variant in CES1.

Patients who carry polymorphisms in CYP2D6 and CES1 that reduce enzymatic activity are at risk of drug related toxicity due to accumulation of toxic by-products and tissue damage (15, 62, 63, 65) but whether METH-PAH patients are carriers of potential pathogenic polymorphisms in these two genes is unknown. We previously published a WES study looking at 12 patients with IPAH where we found TopBp1 as a novel gene modifier in PAH (12). Since then, we have expanded our WES analysis to include 18 unrelated METH-PAH patients who had undergone a complete diagnostic work-up in our Pulmonary Hypertension Clinic over a 5 year period, none of which had any family history of PAH (**Table 1**). These patients reported an average weekly use of METH for 10 years (range: 3 months-25 years) and denied use of other illicit stimulants or anorexinogens. Our patient population was composed predominantly of females (N=11, 62%) with a mean age of 47.8±6.7 years and a body mass index (BMI) of 29.5±3.8. Upon presentation, most patients where categorized as New York Heart Association (NYHA) functional class III (44.4%) and had documented mean six-minute walk distance of 486±145 m. All patients underwent right heart catheterization that showed an average mean right atrial pressure of 10.3±6.3 mmHg, a mean PAP of 51.8±15.8 mmHg, mean PAWP of 11.4±4.5 mmHg,

mean cardiac output of 4.2±1.0 L/min and PVR of 10.7±6.0 WU.

After filtering the WES dataset of METH-PAH patients for synonymous variants, we found a total 10,072 single nucleotide variants (SNV) and 737 Insertion-deletions (i.e. Indels) predicted to affect an estimated total of 1,767 genes. Review of WES data from IPAH and METH-PAH patients led to the identification of six potentially pathogenic CYP2D6 SNVs, predicted to produce missense variants in the protein (**Table 2**). While clinically significant reduction in CYP2D6 enzymatic activity has been documented with rs1135840, rs16947 and rs5030867 (54), only the rs1135840 variant was slightly more prominent in METH-PAH (82.3%) compared to IPAH patients (64%). Regarding CES1, we found five SNVs, two of which were present in both METH-PAH and IPAH patients (**Table 3**). While all three CES1 SNVs fall in highly conserved residues, rs115629050 was exclusively found in METH-PAH patients. Interestingly, this variant is predicted to produce a missense variant located within the active site of the enzyme raising the possibility that it could adversely affect its detoxifying properties.

The CES1 rs115629050 SNV is associated with reduced enzymatic activity and susceptibility to METH induced apoptosis.

The CES1 SNVs known to reduce enzymatic activity have been associated with cocaine and methylphenidate toxicity stressing the importance of intact enzymatic activity to

protect against toxin related injury (15, 65). To test whether METH-PAH carriers of the rs115629050 SNV exhibit reduced CES1 enzymatic activity, we isolated CES1 from PBMCs obtained from ten METH-PAH patients that participated in our WES analysis and measured enzymatic activity by quantifying the rate of 4-nitrophenol (4-NP) hydrolysis, a well-established method to quantify CES1 activity in cells and tissues (45, 60). After controlling for protein amount, we found that CES1 activity was significantly reduced in CES1 rs115629050 SNV positive METH-PAH patients compared to healthy donors (**Fig. 4A**).

Next, we sought to assess whether the rs115629050 CES1 SNV was also present in explanted lung tissues of the four METH-PAH patients presented in Figure 1. We chose these four patients since they were not part of the WES analysis cohort and would serve as a validation cohort for detection of the CES1 SNV. We performed an allelic discrimination assay to screen for the rs115629050 CES1 SNV in DNA extracted from the lung sections. Our analysis demonstrated that two of these four patients (50%) were positive for the rs115629050 whereas both controls, two IPAH and the remaining two METH-PAH patients were negative for this SNV (**Fig. 4B**). With this evidence, we sought to characterize the biological impact of the rs115629050 CES1 mutant allele on PMVEC survival after METH exposure.

Apoptosis is a major consequence of METH exposure and is associated with neuronal cell death and disruption of endothelial blood brain barrier (34, 66) but no study has looked at PMVECs. To test this, we obtained a plasmid containing a wild type (WT) CES1 construct

and generated the rs115629050 mutant using site directed mutagenesis. In the presence of 5 mM METH, PMVECs transfected with the WT CES1 construct demonstrated similar levels of Caspase 3/7 activity as cells transfected with the empty vector (**Fig. 4C**). In contrast, cells transfected with the mutant CES1 plasmid were more vulnerable to METH induced apoptosis as evidenced by significantly higher Caspase 3/7 activity (**Fig. 4C**). Interestingly, in the absence of METH, cells transfected with mutant CES1 had a significant increase in Caspase 3/7 activity as well as a reduced number of viable cells 24 hours after transfection (data not shown), suggesting that either CES1 deficiency or reduced activity can also reduce cell viability. Taken together, these studies support a protective role for CES1 in PMVECs exposed to METH and the CES1 rs115629050 variant appears to reduce this protection.

CES1 reduction leads to increased ROS production and abnormal autophagy flux in METH exposed PMVECs.

Given reduced expression of CES1 in the endothelium of vascular lesions in all four METH-PAH patients, we decided to characterize the consequences of reduced CES1 expression on PMVEC survival with METH exposure. Similar to PMVECs transfected with the mutant CES1 plasmid, CES1 siRNA treated PMVECs (**Fig. 5A**) demonstrate a significant increase in Caspase 3/7 activation in response to 5mM METH as well as a modest increase at baseline (**Fig. 5B**). CYP2D6 siRNA treated PMVECs (**Fig. 5C**) also had significantly more Caspase 3/7 activation in both the METH exposed and non-exposed groups (**Fig. 5D**). This led us to conclude that reduction in either CES1

expression or activity results in reduced PMVEC viability that is further compounded by METH exposure.

We next proceeded to explore the mechanism by which CES1 regulates PMVEC survival against METH. Studies in neurons and brain endothelial cells have shown that METH triggers production of reactive oxygen species (ROS) (11, 50) that results in activation of the autophagy response (3, 42, 44, 64). Autophagy is a process by which the cell degrades and recycles damaged cytoplasmic components in an effort to help the cell cope with stress and restore homeostasis; should these efforts fail, the apoptosis cascade is triggered and cell death ensues. We sought to document whether these events also take place in PMVECs in response to METH exposure and whether loss of CES1 compromises autophagy.

Following METH treatment, we saw an increase in cytoplasmic ROS in both cell groups; however, intensity of ROS signal was significantly stronger in CES1 siRNA treated PMVECs (**Fig. 6A)**. Interestingly, the cytoplasm of METH exposed cells exhibited presence of numerous vacuoles, which appear to be more numerous in CES1 siRNA treated PMVECs. Vacuolization has been previously documented in neurons and endothelial cells exposed to METH and appear to correlate pathologically to organelle swelling and autophagy. We assessed autophagy by measuring autophagic flux, an approach that captures the entire process of autophagy including the delivery of cargo to lysosomes and its subsequent breakdown, through changes in cellular levels of LC3, a cytosolic protein that at baseline (LC3-I) exists as a 18 kDa form but, during autophagy, is

conjugated to form LC3-II and recruited to autophagosomes. In control cells, METH treatment resulted in an increase of LC3-II (**Fig. 6B, left panel**); however, CES1 siRNA treated PMVECs demonstrated a significant LC3-II reduction (**Fig. 6B, right panel).**

To determine whether the changes in LC3-II are determined by changes in autophagic flux, we treated cells with bafilomycin A1, an antibiotic that prevents degradation of autophagosomes by reducing their fusion with lysosomes(35). In control cells, bafilomycin alone resulted in an increase of LC3-II whereas addition of METH resulted in a mild reduction in LC3-II (**Fig. 6C, left panel**). In CES1 siRNA treated PMVECs, we also saw an increase in LC3-II with bafilomycin alone but concomitant exposure to METH led to a significant increase in LC3-II (**Fig. 6C, right panel**).

Taken together, these results support activation of autophagy by METH that is altered in CES1 deficient PMVECs by changes in the autophagic flux. Based on these findings, we conclude that CES1 is required for normal autophagy, which could explain the increased susceptibility of PMVECs to apoptosis in the setting of METH exposure (**Fig. 7**).

DISCUSSION

Originally developed as a therapy for a variety of common clinical disorders such as obesity and Parkinson's disease, illegal manufacture and use of METH has risen worldwide over the past two decades (7, 22, 48). The United Nations Office on Drugs and Crime reported in 2007 that approximately 24.7 million people worldwide were addicted to METH, making this a serious public health problem. In 2008, the US government reported that 13 million people over the age of 12 have used METH at some point and 529,000 are estimated to be regular users. The popularity of METH stems from the fact that it can be easily produced from commercially available reagents in local households (aka. METH labs or kitchens) and its relatively low costs compared to other illicit stimulants. Due to its highly addictive nature, METH can easily become a drug of abuse with a tendency to ruin the lives and productivity of young adults currently in high school and college. At the cost of experiencing transient euphoria and subjective bliss, METH abusers are at risk of severe health problems such as HIV infection, liver damage, stroke and premature cardiac diseases. As one of the largest pulmonary hypertension centers in California, we have seen a disturbing rise in the number of patients being diagnosed with METH-PAH (24), forcing us to expand the research efforts dedicated to understanding the clinical history and mechanism of this devastating form of PAH. This study represents, to our knowledge, the first effort to identify candidate genes in METH-PAH and resulted in three important discoveries: 1) PMVECs are capable of metabolizing METH and 2) CYP2D6 and CES1 are expressed in the lung vessels and appear to be necessary for PMVEC protection and 3) reduced CES1 activity can increase susceptibility to METH induced apoptosis. Since

apoptosis contributes to small vessel loss, it is possible that loss of CES1 expression and/or activity could contribute to development of METH-PAH in susceptible individuals.

CES1 belongs to a family of esterases predominantly expressed in the liver where they are engaged in drug and cholesterol metabolism (38). Interest in CES1 biochemistry has piqued considerably in the last 20 years as allosteric modulators and/or compounds that enhance CES1 activity could serve as therapy for organophosphate poisoning and to treat victims of chemical warfare (60). In our study, we found that both CES1 expression and enzymatic activity appear reduced in METH-PAH and could play parallel roles in compromising the capacity of this enzyme for protecting the endothelium against environmental toxins such as METH. While it could be possible that the two variants found in the N-terminal domain of CES1 (rs3826193 and rs3826192) could compromise stability or appropriate localization of the translated protein to the ER, another possibility is epigenetic suppression secondary to METH, which has been described to occur in other cells (30, 41). On the other hand, pathogenic variants that reduce CES1 activity are associated with the risk of life-threatening adverse drug reactions as seen in patients treated with amantadine and users of illicit drugs such as heroin and cocaine (65). While methylphenidate is a well-established substrate of CES1, this is the first time to our knowledge that METH toxicity has been associated with this enzyme. How CES1 assists in neutralizing METH toxicity in the pulmonary endothelium is unclear at this time. Our LC/MS study argues against direct involvement of CES1 in METH metabolism, which could be predicted on account that the METH molecule does not have esters or amide bonds that could serve as substrate for CES1 (57). That being said, recent metabolomics

studies have shown that METH can induce production of many metabolites in brain (36, 61); therefore, it is possible to predict that METH could trigger the generation of ester or amide containing toxic metabolites in PMVECs that, in the absence of CES1 activity, may result in cell injury. In support of this, studies in dopaminergic cells demonstrate that METH triggers production of 4-hydroxy-2-nonelal (4-HNE), an oxidative byproduct of polyunsaturated fatty acids that can trigger production of cytotoxic esters (4, 8). As mentioned in our results, LC/MS only provides qualitative information on phase 1 metabolism; a more comprehensive metabolomics study will be required to determine whether CES1 is required to buffer production of toxic esters.

Whole Exome Sequencing (WES) is a next generation sequencing technique that focuses on the coding sequences throughout the genome, which has accelerated the discovery of novel variants associated with both Mendelian and non-Mendelian disorders. It is relevant to point out that we found two METH-PH patients (10.5%) who were carriers of BMPR2 missense variant (rs2228545), which targets a residue in the cytoplasmic tail. This SNV has been associated with increased risk of colorectal cancer and has been documented to occur in IPAH patients (16). In addition, other variants in several genes associated with the BMP and TGF beta signaling pathways were documented across the entire population (**Table 4**). To date, no study has firmly established an association between BMPR2 variants and D+T PAH although studies performed on patients with fenfluramine associated PAH revealed that 9% of patients demonstrated pathogenic variants in BMPR2 (29). It will be interesting to determine whether screening larger patient populations could serve to further establish whether a functional link exist between CES1 and BMPR2 in

549 METH-PAH.

550

551 METH induced cytotoxicity is linked to oxidative injury by its direct activation of NAPDH
552 oxidase (NOX) and generation of ROS that cause cellular damage (42). Autophagy is
553 part of an effort to promote cell repair and preserve cell viability in response to oxidative
554 stress; however, if the cells can't recover, autophagy can initiate pro-apoptotic signaling
555 cascades. Therefore, activation of autophagy is a double-edged sword that is vulnerable
556 to changes in protein composition of the ER. Our observation of the increased number of
557 vacuoles in CES1-deficient cells raises several interesting mechanistic possibilities that
558 could provide insight into the fundamental mechanism of METH-induced PMVEC
559 apoptosis. Based on our findings, it appears that CES1 deficiency tilts the balance of
560 autophagic flux towards apoptosis in response to METH exposure. One possible
561 explanation is that CES1 could be facilitating the capacity of the ER to contribute to
562 production of autophagosomes and/or alter lysosome function under METH, since CES1 is
563 expressed in both organelles (2, 17, 40, 56).

564

565 Our studies demonstrate that the reduction in CES1 expression and activity increases
566 PMVEC apoptosis alone and in response to METH but several questions remain
567 concerning the mechanism behind METH induced ROS generation, initiation of ER stress
568 and possible impairment of mitochondrial bioenergetics, a well-established feature of other
569 forms of PAH (14, 37, 46). It is worth pointing out that mitochondrial toxicity is also a
570 consequence of METH exposure and could be linked to the autophagy response as these
571 pathways can also interact with the mitochondria to trigger release of cytochrome C and

other pro-apoptotic factors (52, 59). In light of the link between our other gene candidates (HERPUD1, AKAP1) and the mitochondria, we propose to focus future studies on understanding the role played by the mitochondria in integrating the autophagy responses to METH-induced injury. Whether pharmacological agents that restore CES1 or the autophagy response could be clinically relevant in the treatment of METH-PAH remains to be determined.

While we have focused mainly on the characterization of CES1 variants in this study, it is important to stress that CYP2D6 remains a critical candidate that requires more comprehensive characterization. Besides being the major player in METH metabolism, CYP2D6 is also required for metabolizing anorexinogens linked to PAH such as dexfenfluramine and variants that reduce activity could increase toxicity from these compounds (23, 27). Our WES revealed several candidate CYP2D6 variants some of which occurred with increased frequency in both PAH and METH-PAH patients but it is likely that these are influenced by our small patient numbers values and lack of METH users without evidence of cardiopulmonary disease to serve as the proper reference. Our group has initiated discussions with drug rehabilitation programs in California to start collecting clinical data and blood samples to perform future WES studies in this important control population. Another important limitation is the lack of METH-PAH PMVECs available for *in vitro* studies. Unfortunately, we were only able to establish a cell culture from one of the four patients as the others failed to grow *in vitro*. Furthermore, PMVEC cultures from this single METH-PAH could only endure four passages as their growth progressively slowed down. It is worth speculating why these cells may have less growth

potential compared to other PAH isolates as it could provide critical insight into unique phenotypical and molecular attributes of METH-PAH cells and how they could be affecting cell survival. To overcome this obstacle, our group has started using inducible pluripotent stem cells derived from skin biopsies and PBMCs to generate endothelial cells (iPSC-ECs), a promising approach that will hopefully allow us to expand our mechanistic studies of METH-PAH.

In conclusion, we propose a model by which reduced expression and/or reduced CES1 activity could predispose to PAH by increasing susceptibility of PMVECs to METH-induced apoptosis (**Fig. 7**). CES1 holds potential as a biomarker that could be used to identify METH users at risk of developing PAH and as a potential candidate target for agents capable of restoring expression and/or activity, which could then help increase cell viability and reduce disease progression in this population. It is our hope that characterizing CES1 and other genes identified by WES will allow us to increase our chances of identifying high risk individuals and improve our capacity to better care for those who suffer from this devastating disease. While the findings presented here are pertinent to METH-PAH, we anticipate that our findings will serve to open the field for investigations that will seek to uncover deeper links between gene interactions and other relevant exposures associated with D+T PAH.

ACKNOWLEDGEMENTS

Lung tissues from IPAH and control patients were provided by the Pulmonary Hypertension Breakthrough Initiative, which is funded by the Cardiovascular Medical Research and Education Fund (CMREF) and managed at Stanford by Drs. Marlene Rabinovitch and Roham T. Zamanian. The tissues were procured at the Transplant Procurement Centers at Stanford University, Cleveland Clinic, and Allegheny General Hospital and de-identified patient data were obtained via the Data Coordinating Center at the University of Michigan. The authors thank all patients and their proxies who participated in this study. The authors are also grateful to Patricia Angeles del Rosario for helping with the collection and processing of blood samples and Mr. Andrew Hsi for helping organize the patient database.

AUTHOR DISCLOSURES

R.T. Zamanian has served as consultant for United Therapeutics, Actelion, Gilead and Bayer Pharmaceuticals and receives research support from United Therapeutics and Actelion.

FUNDING SOURCES

This work was supported by a seed grant from the Vera Moulton Wall Center, a career development award from the Robert Wood Johnson Foundation, an NIH R01 HL134776, K08 HL105884-01 award, a Pulmonary Hypertension Association, American Lung Association Biomedical Research Grants and American Heart Association Beginning Grant in Aid to V. de Jesus Perez. R.T. Zamanian is supported by funds from NIH NHLBI and NIAID and the Vera Moulton Wall Center. This work was partially funded by the National Institute of Environmental Health Sciences (P42 ES04699). S.D. Kodani is supported by a NIGMS-funded Pharmacology Training Program (T32GM099608). B. Hammock is supported by an NIEHS R01 ES002710 grant.

REFERENCES

1. **Abenhaim L, Moride Y, Brenot F, Rich S, Benichou J, Kurz X, Higenbottam T, Oakley C, Wouters E, Aubier M, Simonneau G, and Begaud B**. Appetite-suppressant drugs and the risk of primary pulmonary hypertension. International Primary Pulmonary Hypertension Study Group. *The New England journal of medicine* 335: 609-616, 1996.
2. **Amouzadeh HR, Bourdi M, Martin JL, Martin BM, and Pohl LR**. UDP-glucose:glycoprotein glucosyltransferase associates with endoplasmic reticulum chaperones and its activity is decreased in vivo by the inhalation anesthetic halothane. *Chem Res Toxicol* 10: 59-63, 1997.

3. **Beauvais G, Atwell K, Jayanthi S, Ladenheim B, and Cadet JL**. Involvement of dopamine receptors in binge methamphetamine-induced activation of endoplasmic reticulum and mitochondrial stress pathways. *PloS one* 6: e28946, 2011.

4. **Borazjani A, Edelmann MJ, Hardin KL, Herring KL, Allen Crow J, and Ross MK**. Catabolism of 4-hydroxy-2-trans-nonenal by THP1 monocytes/macrophages and inactivation of carboxylesterases by this lipid electrophile. *Chemico-biological interactions* 194: 1-12, 2011.

5. **Brenot F, Herve P, Petitpretz P, Parent F, Duroux P, and Simonneau G**. Primary pulmonary hypertension and fenfluramine use. *British heart journal* 70: 537-541, 1993.

6. **Bruxel EM, Salatino-Oliveira A, Genro JP, Zeni CP, Polanczyk GV, Chazan R, Rohde LA, and Hutz MH**. Association of a carboxylesterase 1 polymorphism with appetite reduction in children and adolescents with attention-deficit/hyperactivity disorder treated with methylphenidate. *The pharmacogenomics journal* 13: 476-480, 2013.

7. **Calcaterra S, and Binswanger IA**. National trends in psychostimulant-related deaths: 1999-2009. *Substance abuse* 34: 129-136, 2013.

8. **Chandramani Shivalingappa P, Jin H, Anantharam V, Kanthasamy A, and Kanthasamy A**. N-Acetyl Cysteine Protects against Methamphetamine-Induced Dopaminergic Neurodegeneration via Modulation of Redox Status and Autophagy in Dopaminergic Cells. *Parkinson's disease* 2012: 424285, 2012.

9. **Cherner M, Bousman C, Everall I, Barron D, Letendre S, Vaida F, Atkinson JH, Heaton R, Grant I, and Group H**. Cytochrome P450-2D6 extensive metabolizers are more vulnerable to methamphetamine-associated neurocognitive impairment: preliminary findings. *Journal of the International Neuropsychological Society : JINS* 16: 890-901, 2010.

10. **Chin KM, Channick RN, and Rubin LJ**. Is methamphetamine use associated with idiopathic pulmonary arterial hypertension? *Chest* 130: 1657-1663, 2006.

11. **da Silva DD, Silva E, and Carmo H**. Combination effects of amphetamines under hyperthermia - the role played by oxidative stress. *Journal of applied toxicology : JAT* 34: 637-650, 2014.

12. **de Jesus Perez VA, Yuan K, Lyuksyutova MA, Dewey F, Orcholski ME, Shuffle EM, Mathur M, Yancy L, Jr., Rojas V, Li CG, Cao A, Alastalo TP, Khazeni N, Cimprich KA, Butte AJ, Ashley E, and Zamanian RT**. Whole-exome sequencing reveals TopBP1 as a novel gene in idiopathic pulmonary arterial hypertension. *American journal of respiratory and critical care medicine* 189: 1260-1272, 2014.

13. **de la Torre R, Yubero-Lahoz S, Pardo-Lozano R, and Farre M**. MDMA, methamphetamine, and CYP2D6 pharmacogenetics: what is clinically relevant? *Frontiers in genetics* 3: 235, 2012.

14. **Dunham-Snary KJ, Hong ZG, Xiong PY, Del Paggio JC, Herr JE, Johri AM, and Archer SL**. A mitochondrial redox oxygen sensor in the pulmonary vasculature and ductus arteriosus. *Pflugers Archiv : European journal of physiology* 468: 43-58, 2016.

15. **Duysen EG, and Lockridge O**. Prolonged toxic effects after cocaine challenge in butyrylcholinesterase/plasma carboxylesterase double knockout mice: a model for butyrylcholinesterase-deficient humans. *Drug metabolism and disposition: the biological fate of chemicals* 39: 1321-1323, 2011.

16. **Elliott CG, Glissmeyer EW, Havlena GT, Carlquist J, McKinney JT, Rich S, McGoon MD, Scholand MB, Kim M, Jensen RL, Schmidt JW, and Ward K**. Relationship of

728 BMPR2 mutations to vasoreactivity in pulmonary arterial hypertension. *Circulation* 113:
729 2509-2515, 2006.
730 17. **Funakoshi-Hirose I, Aki T, Unuma K, Funakoshi T, Noritake K, and Uemura K**. Distinct
731 effects of methamphetamine on autophagy-lysosome and ubiquitin-proteasome systems in
732 HL-1 cultured mouse atrial cardiomyocytes. *Toxicology* 312: 74-82, 2013.
733 18. **Galie N, Hoeper MM, Humbert M, Torbicki A, Vachiery JL, Barbera JA, Beghetti M,**
734 **Corris P, Gaine S, Gibbs JS, Gomez-Sanchez MA, Jondeau G, Klepetko W, Opitz C,**
735 **Peacock A, Rubin L, Zellweger M, and Simonneau G**. Guidelines for the diagnosis and
736 treatment of pulmonary hypertension. *The European respiratory journal* 34: 1219-1263,
737 2009.
738 19. **Galie N, Humbert M, Vachiery JL, Gibbs S, Lang I, Torbicki A, Simonneau G,**
739 **Peacock A, Vonk Noordegraaf A, Beghetti M, Ghofrani A, Gomez Sanchez MA,**
740 **Hansmann G, Klepetko W, Lancellotti P, Matucci M, McDonagh T, Pierard LA,**
741 **Trindade PT, Zompatori M, Hoeper M, Aboyans V, Vaz Carneiro A, Achenbach S,**
742 **Agewall S, Allanore Y, Asteggiano R, Paolo Badano L, Albert Barbera J, Bouvaist H,**
743 **Bueno H, Byrne RA, Carerj S, Castro G, Erol C, Falk V, Funck-Brentano C, Gorenflo**
744 **M, Granton J, Iung B, Kiely DG, Kirchhof P, Kjellstrom B, Landmesser U, Lekakis J,**
745 **Lionis C, Lip GY, Orfanos SE, Park MH, Piepoli MF, Ponikowski P, Revel MP, Rigau**
746 **D, Rosenkranz S, Voller H, and Luis Zamorano J**. 2015 ESC/ERS Guidelines for the
747 diagnosis and treatment of pulmonary hypertension: The Joint Task Force for the
748 Diagnosis and Treatment of Pulmonary Hypertension of the European Society of
749 Cardiology (ESC) and the European Respiratory Society (ERS): Endorsed by: Association

for European Paediatric and Congenital Cardiology (AEPC), International Society for Heart and Lung Transplantation (ISHLT). *European heart journal* 37: 67-119, 2016.

20. **Galie N, and Simonneau G**. The Fifth World Symposium on Pulmonary Hypertension. *Journal of the American College of Cardiology* 62: D1-3, 2013.

21. **Gotway MB, Marder SR, Hanks DK, Leung JW, Dawn SK, Gean AD, Reddy GP, Araoz PA, and Webb WR**. Thoracic complications of illicit drug use: an organ system approach. *Radiographics : a review publication of the Radiological Society of North America, Inc* 22 Spec No: S119-135, 2002.

22. **Greberman SB, and Wada K**. Social and legal factors related to drug abuse in the United States and Japan. *Public health reports* 109: 731-737, 1994.

23. **Gross AS, Phillips AC, Rieutord A, and Shenfield GM**. The influence of the sparteine/debrisoquine genetic polymorphism on the disposition of dexfenfluramine. *British journal of clinical pharmacology* 41: 311-317, 1996.

24. **Gruenewald PJ, Ponicki WR, Remer LG, Waller LA, Zhu L, and Gorman DM**. Mapping the spread of methamphetamine abuse in California from 1995 to 2008. *American journal of public health* 103: 1262-1270, 2013.

25. **Guidice JM, Marez D, Sabbagh N, Legrand-Andreoletti M, Spire C, Alcaide E, Lafitte JJ, and Broly F**. Evidence for CYP2D6 expression in human lung. *Biochemical and biophysical research communications* 241: 79-85, 1997.

26. **Gurney MA, Huang C, Ramil JM, Ravindran N, Andres AM, Sin J, Linton PJ, and Gottlieb RA**. Measuring cardiac autophagic flux in vitro and in vivo. *Methods in molecular biology* 1219: 187-197, 2015.

27. **Haritos VS, Ching MS, Ghabrial H, Gross AS, Taavitsainen P, Pelkonen O, Battaglia SE, Smallwood RA, and Ahokas JT**. Metabolism of dexfenfluramine in human liver microsomes and by recombinant enzymes: role of CYP2D6 and 1A2. *Pharmacogenetics* 8: 423-432, 1998.

28. **Hatfield MJ, Umans RA, Hyatt JL, Edwards CC, Wierdl M, Tsurkan L, Taylor MR, and Potter PM**. Carboxylesterases: General detoxifying enzymes. *Chemico-biological interactions* 2016.

29. **Humbert M, Deng Z, Simonneau G, Barst RJ, Sitbon O, Wolf M, Cuervo N, Moore KJ, Hodge SE, Knowles JA, and Morse JH**. BMPR2 germline mutations in pulmonary hypertension associated with fenfluramine derivatives. *The European respiratory journal* 20: 518-523, 2002.

30. **Itzhak Y, Ergui I, and Young JI**. Long-term parental methamphetamine exposure of mice influences behavior and hippocampal DNA methylation of the offspring. *Molecular psychiatry* 20: 232-239, 2015.

31. **Krupp M, Marquardt JU, Sahin U, Galle PR, Castle J, and Teufel A**. RNA-Seq Atlas--a reference database for gene expression profiling in normal tissue by next-generation sequencing. *Bioinformatics* 28: 1184-1185, 2012.

32. **Laizure SC, Herring V, Hu Z, Witbrodt K, and Parker RB**. The role of human carboxylesterases in drug metabolism: have we overlooked their importance? *Pharmacotherapy* 33: 210-222, 2013.

33. **Lin LY, Di Stefano EW, Schmitz DA, Hsu L, Ellis SW, Lennard MS, Tucker GT, and Cho AK**. Oxidation of methamphetamine and methylenedioxymethamphetamine by

CYP2D6. *Drug metabolism and disposition: the biological fate of chemicals* 25: 1059-1064, 1997.

34. **Ma J, Wan J, Meng J, Banerjee S, Ramakrishnan S, and Roy S**. Methamphetamine induces autophagy as a pro-survival response against apoptotic endothelial cell death through the Kappa opioid receptor. *Cell death & disease* 5: e1099, 2014.

35. **Mauvezin C, and Neufeld TP**. Bafilomycin A1 disrupts autophagic flux by inhibiting both V-ATPase-dependent acidification and Ca-P60A/SERCA-dependent autophagosome-lysosome fusion. *Autophagy* 11: 1437-1438, 2015.

36. **McClay JL, Adkins DE, Vunck SA, Batman AM, Vann RE, Clark SL, Beardsley PM, and van den Oord EJ**. Large-scale neurochemical metabolomics analysis identifies multiple compounds associated with methamphetamine exposure. *Metabolomics : Official journal of the Metabolomic Society* 9: 392-402, 2013.

37. **McMurtry MS, Archer SL, Altieri DC, Bonnet S, Haromy A, Harry G, Bonnet S, Puttagunta L, and Michelakis ED**. Gene therapy targeting survivin selectively induces pulmonary vascular apoptosis and reverses pulmonary arterial hypertension. *The Journal of clinical investigation* 115: 1479-1491, 2005.

38. **Merali Z, Ross S, and Pare G**. The pharmacogenetics of carboxylesterases: CES1 and CES2 genetic variants and their clinical effect. *Drug metabolism and drug interactions* 29: 143-151, 2014.

39. **Nemoda Z, Angyal N, Tarnok Z, Gadoros J, and Sasvari-Szekely M**. Carboxylesterase 1 gene polymorphism and methylphenidate response in ADHD. *Neuropharmacology* 57: 731-733, 2009.

40. **Nousiainen U, and Torronen R**. Differentiation of microsomal and cytosolic carboxylesterases in the rat liver by in vivo and in vitro inhibition. *General pharmacology* 15: 223-227, 1984.

41. **Numachi Y, Shen H, Yoshida S, Fujiyama K, Toda S, Matsuoka H, Sora I, and Sato M**. Methamphetamine alters expression of DNA methyltransferase 1 mRNA in rat brain. *Neuroscience letters* 414: 213-217, 2007.

42. **Park M, Hennig B, and Toborek M**. Methamphetamine alters occludin expression via NADPH oxidase-induced oxidative insult and intact caveolae. *Journal of cellular and molecular medicine* 16: 362-375, 2012.

43. **Rabinovitch M**. Molecular pathogenesis of pulmonary arterial hypertension. *The Journal of clinical investigation* 122: 4306-4313, 2012.

44. **Ramirez SH, Potula R, Fan S, Eidem T, Papugani A, Reichenbach N, Dykstra H, Weksler BB, Romero IA, Couraud PO, and Persidsky Y**. Methamphetamine disrupts blood-brain barrier function by induction of oxidative stress in brain endothelial cells. *Journal of cerebral blood flow and metabolism : official journal of the International Society of Cerebral Blood Flow and Metabolism* 29: 1933-1945, 2009.

45. **Rayo J, Munoz L, Rosell G, Hammock BD, Guerrero A, Luque FJ, and Pouplana R**. Reactivity versus steric effects in fluorinated ketones as esterase inhibitors: a quantum mechanical and molecular dynamics study. *Journal of molecular modeling* 16: 1753-1764, 2010.

46. **Rehman J, and Archer SL**. A proposed mitochondrial-metabolic mechanism for initiation and maintenance of pulmonary arterial hypertension in fawn-hooded rats: the Warburg

model of pulmonary arterial hypertension. *Advances in experimental medicine and biology* 661: 171-185, 2010.

47. **Rich S, Rubin L, Walker AM, Schneeweiss S, and Abenhaim L**. Anorexigens and pulmonary hypertension in the United States: results from the surveillance of North American pulmonary hypertension. *Chest* 117: 870-874, 2000.

48. **Richards JR, Bretz SW, Johnson EB, Turnipseed SD, Brofeldt BT, and Derlet RW**. Methamphetamine abuse and emergency department utilization. *The Western journal of medicine* 170: 198-202, 1999.

49. **Sa S, Gu M, Chappell J, Shao NY, Ameen M, Elliott KA, Li D, Grubert F, Li CG, Taylor S, Cao A, Ma Y, Fong R, Nguyen L, Wu JC, Snyder MP, and Rabinovitch M**. Induced Pluripotent Stem Cell Model of Pulmonary Arterial Hypertension Reveals Novel Gene Expression and Patient Specificity. *American journal of respiratory and critical care medicine* 195: 930-941, 2017.

50. **Sajja RK, Rahman S, and Cucullo L**. Drugs of abuse and blood-brain barrier endothelial dysfunction: A focus on the role of oxidative stress. *Journal of cerebral blood flow and metabolism : official journal of the International Society of Cerebral Blood Flow and Metabolism* 2015.

51. **Schaiberger PH, Kennedy TC, Miller FC, Gal J, and Petty TL**. Pulmonary hypertension associated with long-term inhalation of "crank" methamphetamine. *Chest* 104: 614-616, 1993.

52. **Senft D, and Ronai ZA**. UPR, autophagy, and mitochondria crosstalk underlies the ER stress response. *Trends in biochemical sciences* 40: 141-148, 2015.

53. **Shima N, Tsutsumi H, Kamata T, Nishikawa M, Katagi M, Miki A, and Tsuchihashi H**. Direct determination of glucuronide and sulfate of p-hydroxymethamphetamine in methamphetamine users' urine. *Journal of chromatography B, Analytical technologies in the biomedical and life sciences* 830: 64-70, 2006.

54. **Solus JF, Arietta BJ, Harris JR, Sexton DP, Steward JQ, McMunn C, Ihrie P, Mehall JM, Edwards TL, and Dawson EP**. Genetic variation in eleven phase I drug metabolism genes in an ethnically diverse population. *Pharmacogenomics* 5: 895-931, 2004.

55. **Sun Z, Murry DJ, Sanghani SP, Davis WI, Kedishvili NY, Zou Q, Hurley TD, and Bosron WF**. Methylphenidate is stereoselectively hydrolyzed by human carboxylesterase CES1A1. *The Journal of pharmacology and experimental therapeutics* 310: 469-476, 2004.

56. **Tanaka M, Iio T, and Tabata T**. Purification and characterization of a carboxylesterase from rabbit liver lysosomes. *Journal of biochemistry* 101: 619-624, 1987.

57. **Thomsen R, Rasmussen HB, Linnet K, and Consortium I**. In vitro drug metabolism by human carboxylesterase 1: focus on angiotensin-converting enzyme inhibitors. *Drug metabolism and disposition: the biological fate of chemicals* 42: 126-133, 2014.

58. **Volkow ND, Fowler JS, Wang GJ, Shumay E, Telang F, Thanos PK, and Alexoff D**. Distribution and pharmacokinetics of methamphetamine in the human body: clinical implications. *PloS one* 5: e15269, 2010.

59. **Walter L, and Hajnoczky G**. Mitochondria and endoplasmic reticulum: the lethal interorganelle cross-talk. *Journal of bioenergetics and biomembranes* 37: 191-206, 2005.

60. **Williams ET, Bacon JA, Bender DM, Lowinger JJ, Guo WK, Ehsani ME, Wang X, Wang H, Qian YW, Ruterbories KJ, Wrighton SA, and Perkins EJ**. Characterization of the expression and activity of carboxylesterases 1 and 2 from the beagle dog, cynomolgus

monkey, and human. *Drug metabolism and disposition: the biological fate of chemicals* 39: 2305-2313, 2011.

61. **Zaitsu K, Hayashi Y, Kusano M, Tsuchihashi H, and Ishii A**. Application of metabolomics to toxicology of drugs of abuse: A mini review of metabolomics approach to acute and chronic toxicity studies. *Drug metabolism and pharmacokinetics* 31: 21-26, 2016.

62. **Zanger UM, Raimundo S, and Eichelbaum M**. Cytochrome P450 2D6: overview and update on pharmacology, genetics, biochemistry. *Naunyn-Schmiedeberg's archives of pharmacology* 369: 23-37, 2004.

63. **Zanger UM, and Schwab M**. Cytochrome P450 enzymes in drug metabolism: regulation of gene expression, enzyme activities, and impact of genetic variation. *Pharmacology & therapeutics* 138: 103-141, 2013.

64. **Zhang X, Banerjee A, Banks WA, and Ercal N**. N-Acetylcysteine amide protects against methamphetamine-induced oxidative stress and neurotoxicity in immortalized human brain endothelial cells. *Brain research* 1275: 87-95, 2009.

65. **Zhu HJ, Patrick KS, Yuan HJ, Wang JS, Donovan JL, DeVane CL, Malcolm R, Johnson JA, Youngblood GL, Sweet DH, Langaee TY, and Markowitz JS**. Two CES1 gene mutations lead to dysfunctional carboxylesterase 1 activity in man: clinical significance and molecular basis. *American journal of human genetics* 82: 1241-1248, 2008.

66. **Zhu JP, Xu W, and Angulo JA**. Methamphetamine-induced cell death: selective vulnerability in neuronal subpopulations of the striatum in mice. *Neuroscience* 140: 607-622, 2006.

67. **Zhu W, Song L, Zhang H, Matoney L, LeCluyse E, and Yan B**. Dexamethasone differentially regulates expression of carboxylesterase genes in humans and rats. *Drug metabolism and disposition: the biological fate of chemicals* 28: 186-191, 2000.

TABLES AND FIGURES

Figure 1. CES1 expression is reduced in vascular lesions of METH-PAH. (A) Representative immunofluorescence studies of lung sections stained for CYP2D6 (red) obtained from healthy donor and METH-PAH patients. No difference was seen among our four METH-PAH patients. (B) Representative immunofluorescence studies of lung sections stained for CES1 (red) obtained from healthy donor (top) and four METH-PAH patients. CD31 (green) stains for endothelial cells. Scale bar=25μm.

Figure 2. Expression of CYP2D6 and CES1 in lung sections of IPAH, CF and IPF patients. (A-C) Representative immunofluorescence studies of IPAH (A), CF (B) and IPF (C) lung sections stained for CYP2D6 (red). (D-F) Lung sections from IPAH (D), CF (E) and IPF (F) stained for CES1. CD31 (green) stains for endothelial cells. Scale bar=25μm

Figure 3. METH is metabolized by PMVECs into P-OHMA. (A) Diagram illustrating the phase I metabolism of METH into amphetamine (AP) and p-OHMA. P-OHMA could be further metabolized into p-OHMA glucuronide (Glu) and p-OHMA sulfate (Sul) in the liver to increase solubility and facilitate urinary excretion. (B) LC/MS study of PMVECs treated with METH for 4 hours. Analysis of cell lysates demonstrated at least five OHMA metabolites (peaks 2-6). Panel A represents full scan LC-MS chromatograms of treated and untreated samples. Panel B represents CID chromatograms (MS2 m/z 166.2 @CID 35.00) of hydroxylated methamphetamine metabolites in the same samples. Panel C represents MS/MS spectra of METH hydroxymetabolites (peaks 2 through 6). Peak #1 is a nonspecific endogenous component, also found in unstimulated PMVECs.

Figure 4. CES1 rs115629050 variant is associated with reduced enzymatic activity and increased apoptosis in unstimulated and METH exposed PMVECs. (A) CES1 activity assay of PBMCs from healthy donors (WT) and METH-PAH patients carrying the rs115629050. *P<0.05, unpaired t-test. (B) Allelic discrimination assay for rs115629050 in gDNA samples extracted from lung tissue paraffin blocks (see methods). (C) Caspase 3/7 activity assay of PMVECs transfected with either GFP, wild type (CES1) or rs115629050 mutant (Mutant CES1) plasmids. ***P*<0.01 and ****P*<0.001 vs. all other groups; ordinary one-way ANOVA with Tukey's multiple comparisons test.

Figure 5. CES1 and CYP2D6 deficient PMVECs have increased susceptibility to apoptosis. (A) WB for CES1 in control (siCt) or CES siRNA transfected healthy human PMVECs. (B) Caspase 3/7 activity assays of siCt and CES1 siRNA transfected PMVECs at

baseline and following METH (5mM) exposure for 4 hours. (C) WB and caspase 3/7 assay (D) for CYP2D6 in siCt or CYP2D6 (si2D6) siRNA transfected healthy human PMVECs. Numbers under WB represent densitometry ratio of signal vs. tubulin from 3 independent studies. *P<0.05 and ***P<0.001; ordinary one-way ANOVA with Tukey's multiple comparisons test.

Figure 6. CES1 deficient PMVECs demonstrate reduced autophagy in response to METH. (A) Non-exposed and 4-hour METH exposed control (siCt) and CES1 (siCES1) siRNA treated cells were fixed and stained with CellRox green. Fluorescence was measured relative to Ctrl-no METH. ***P<0.0001, unpaired t-test. (B) WB of unstimulated and 4 hr-METH Ctrll and siCES1 treated cells for LC3. (C) WB of bafilomycin treated unstimulated and 4 hr-METH treated Ctrl and siCES1 cells for LC3. Densitometry is measured relative to □-tubulin as a loading control. ***P<0.0001 vs. Ctrl-no METH. ##P<0.001 vs. corresponding control, one-way ANOVA with Bonferroni post test (N=3).

Figure 7. Proposed Model. METH enters PMVECs and is metabolized to p-OHMA and other toxic metabolites, which trigger ROS production and an autophagy response. CES1 (green) is required to reduce ROS production and maintain steady autophagy flux. Reduced CES1 expression and/or activity (red) result in increased ROS production and abnormal autophagy flux, resulting in increased PMVEC apoptosis and loss of pulmonary microvessels.

Table 1. Patient Characteristics of METH-PAH patients involved in WES.

Table 2. Predicted amino acid location and functional impact of CYP2D6 variants found in WES of IPAH and METH-PAH patients.

Table 3. Predicted amino acid location and functional impact of CES1 variants found in WES of IPAH and METH-PAH patients.

Table 4. Variants found in genes involved in the BMP signaling pathway via WES.

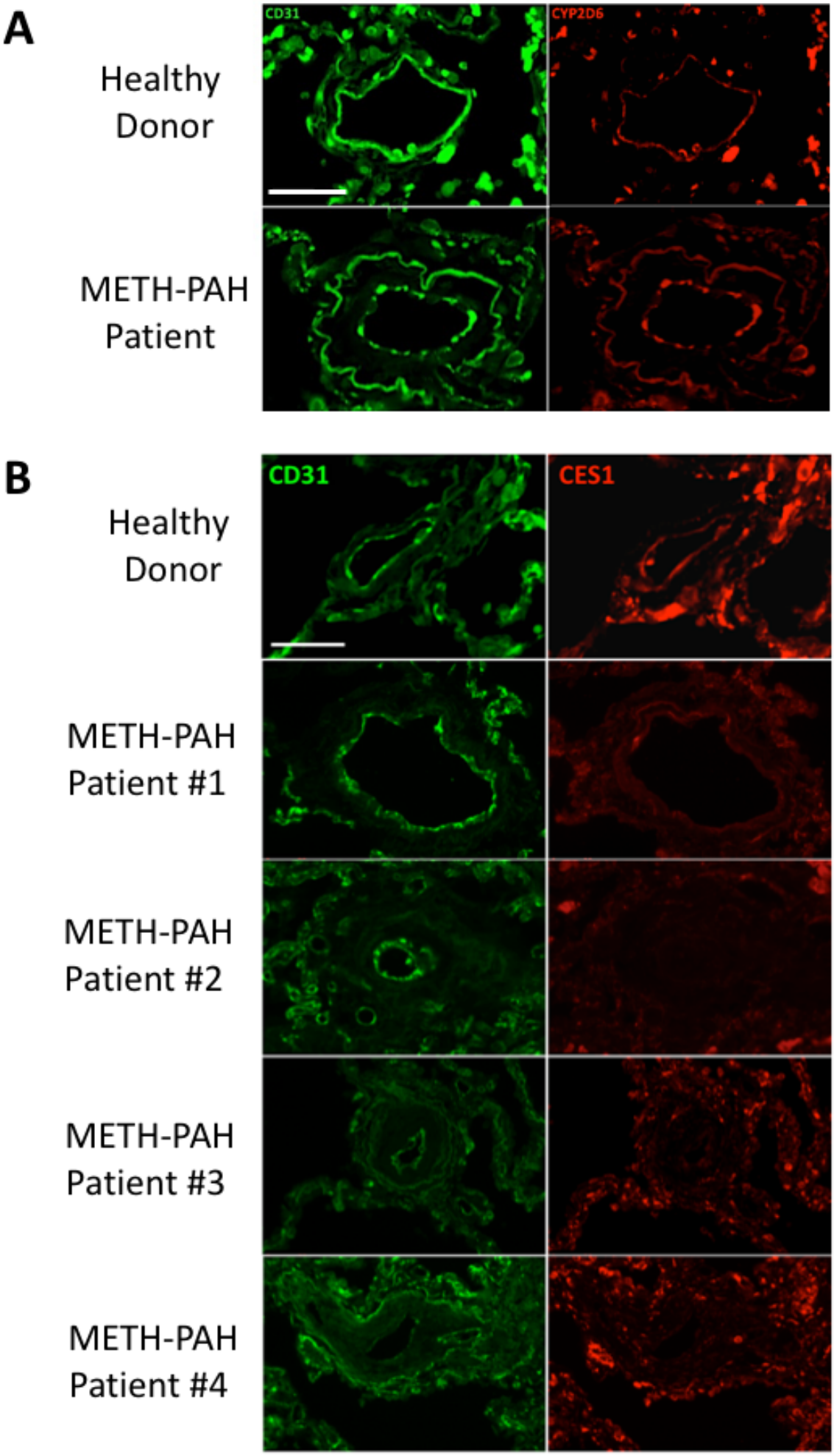
A
Healthy Donor
METH-PAH Patient
CD31
CYP2D6
B
Healthy Donor
METH-PAH Patient #1
METH-PAH Patient #2
METH-PAH Patient #3
METH-PAH Patient #4
CD31
CES1

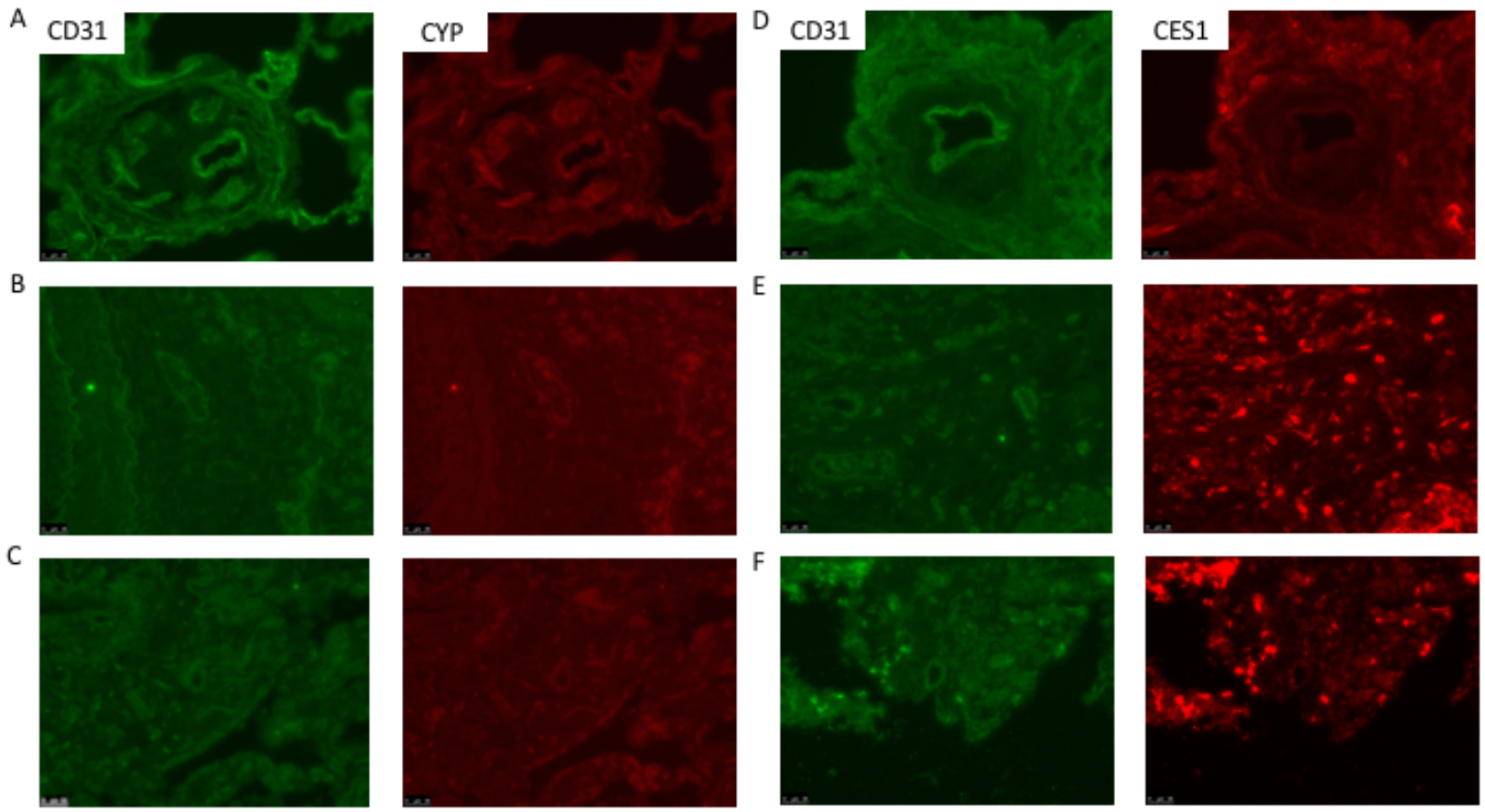
A
CD31
CYP
D
CD31
CES1
B
E
C
F

A

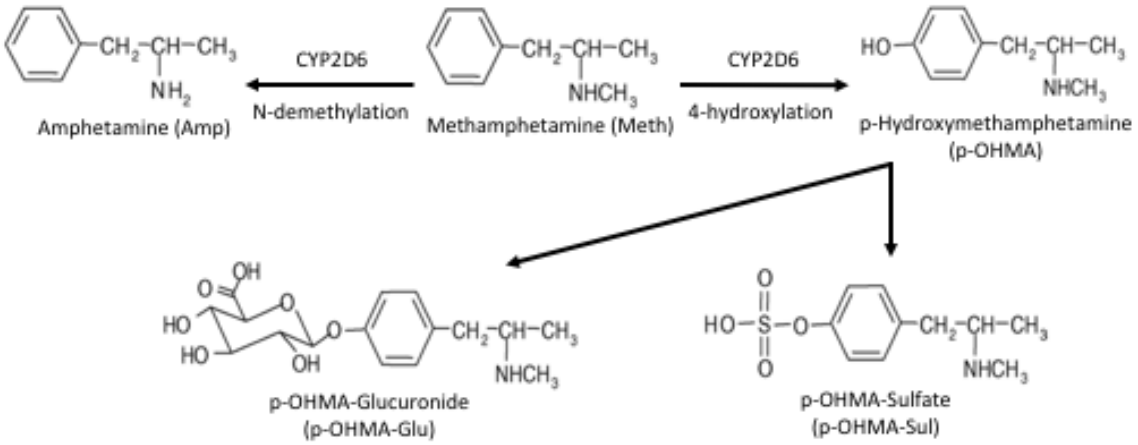
CYP2D6
N-demethylation
CYP2D6
4-hydroxylation
Amphetamine (Amp)
Methamphetamine (Meth)
p-Hydroxymethamphetamine
(p-OHMA)
p-OHMA-Glucuronide
(p-OHMA-Glu)
p-OHMA-Sulfate
(p-OHMA-Sul)

B

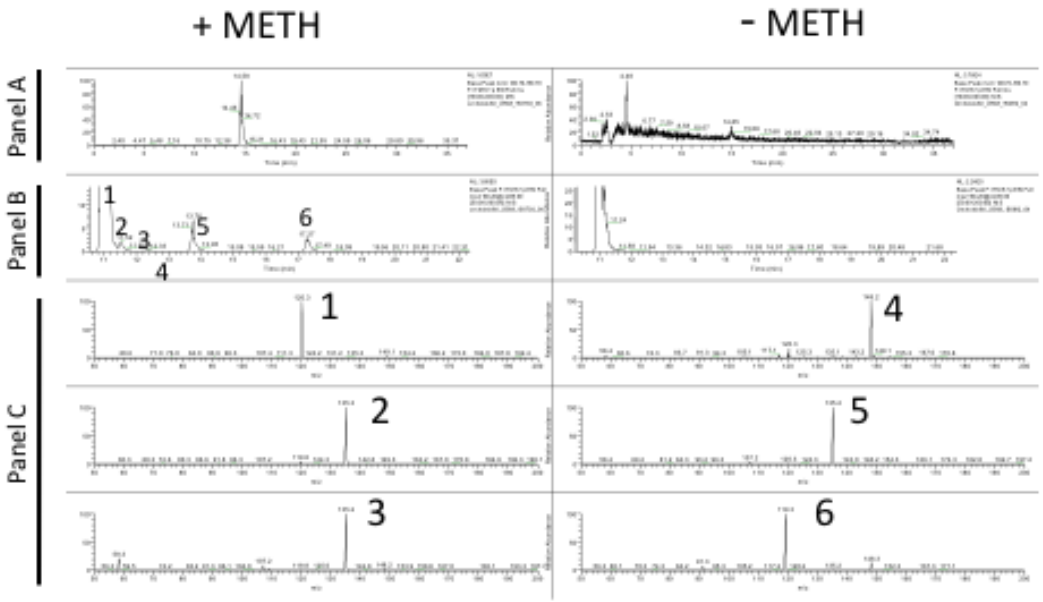
+ METH
- METH
Panel A
Panel B
Panel C
1
2
3
4
5
6

A

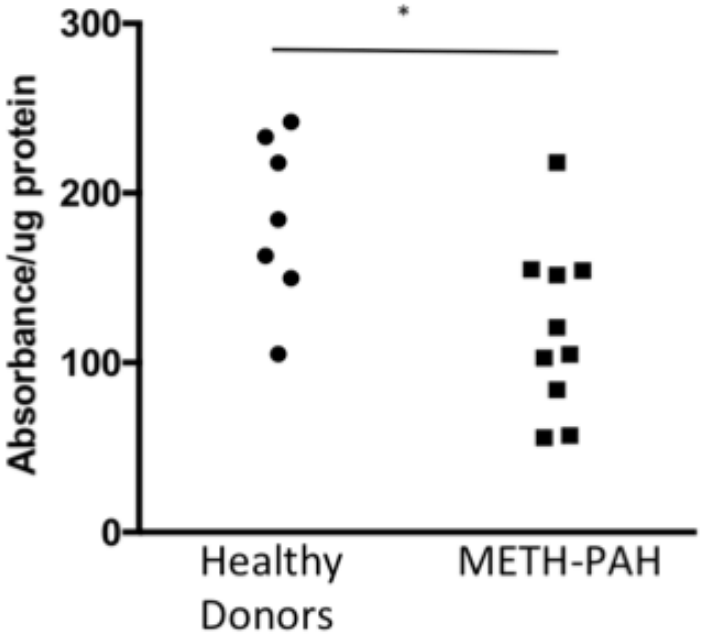

B

Wild Type Allele	C
SNP ID	rs115629050
Meth-PH 1	C/A
Meth-PH 2	C/A
Meth-PH 3	C/C
Meth-PH 4	C/C
PH 1	C/C
PH 2	C/C
Healthy 1	C/C
Healthy 2	C/C

C

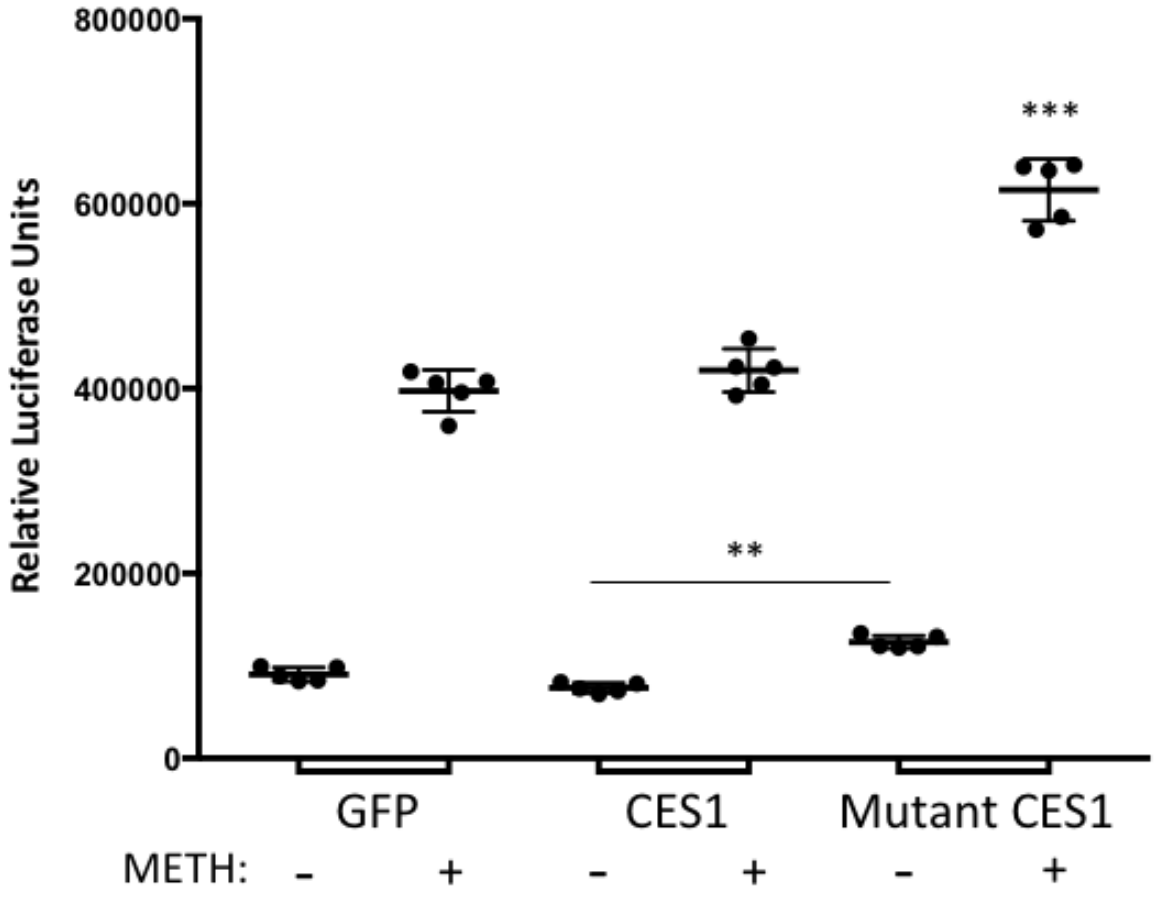

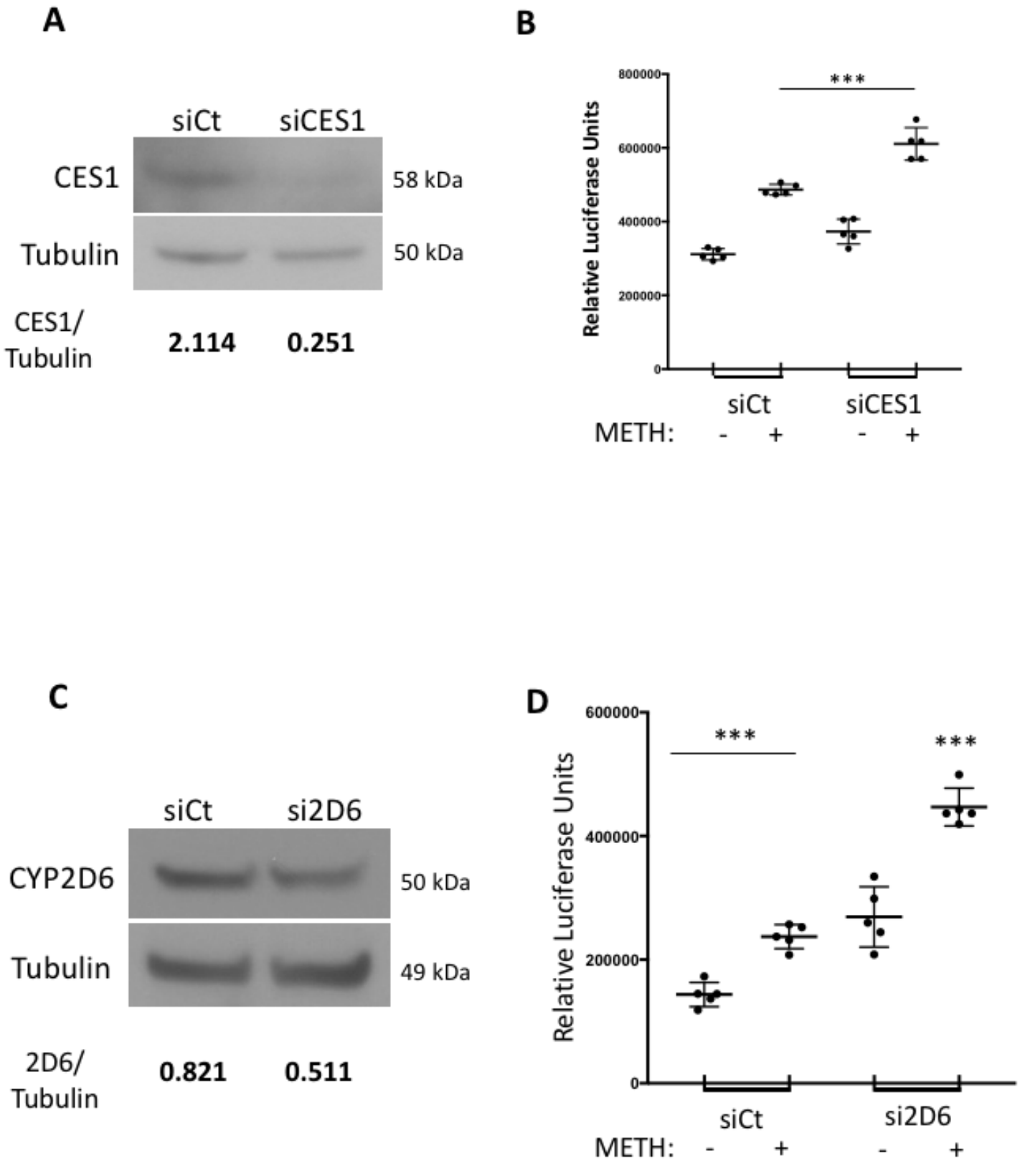
A
siCt
siCES1
CES1
58 kDa
Tubulin
50 kDa
CES1/
Tubulin
2.114
0.251
B
Relative Luciferase Units
800000
600000
400000
200000
0
***
siCt
siCES1
METH: - + - +
C
siCt
si2D6
CYP2D6
50 kDa
Tubulin
49 kDa
2D6/
Tubulin
0.821
0.511
D
Relative Luciferase Units
600000
400000
200000
0
***
***
siCt
si2D6
METH: - + - +

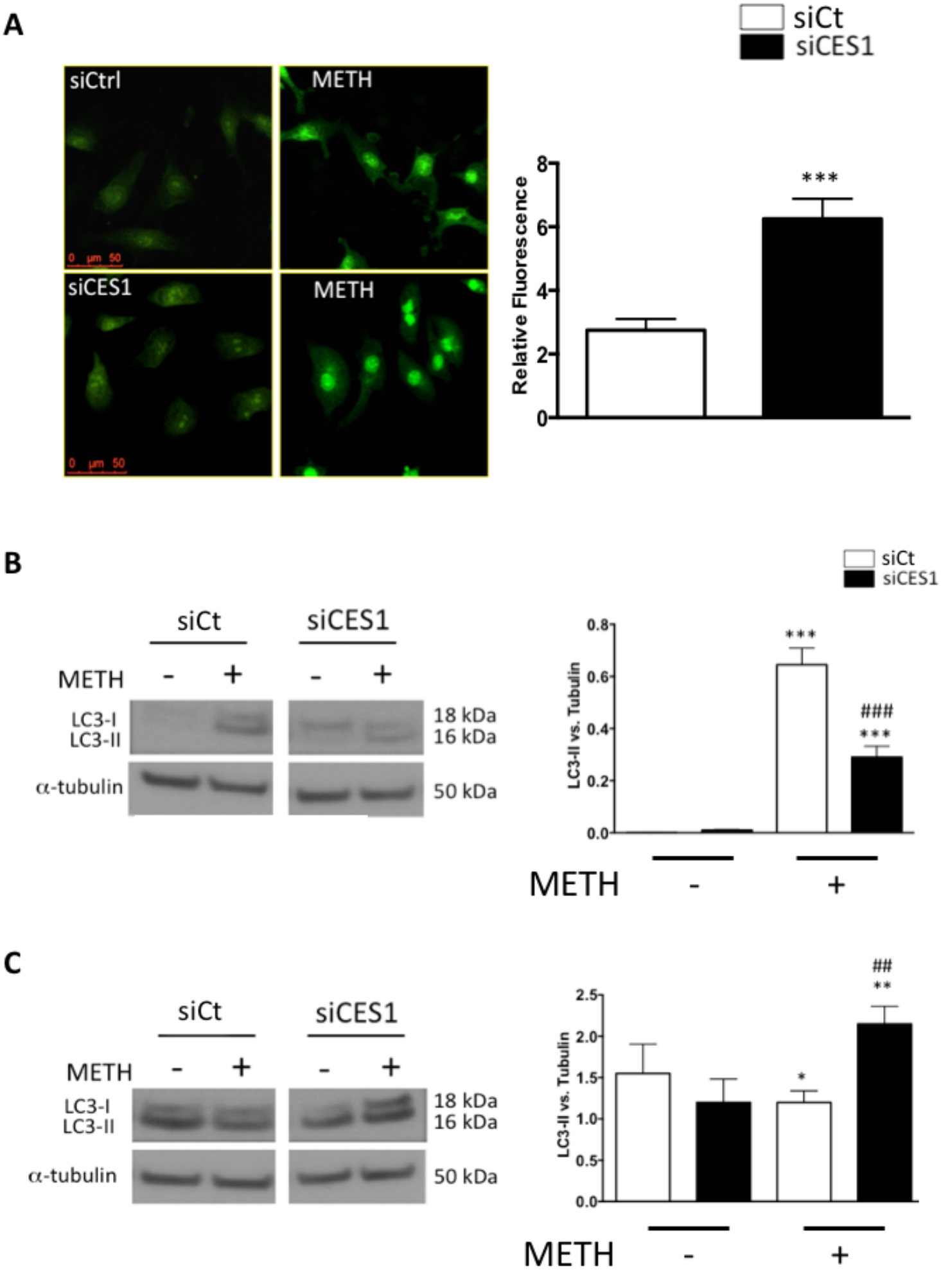
A
siCt
siCES1
siCtrl
METH
siCES1
METH
0 µm 50
0 µm 50
Relative Fluorescence
8
6
4
2
0
***
B
siCt
siCES1
siCt
siCES1
METH - + - +
LC3-I
LC3-II
18 kDa
16 kDa
α-tubulin
50 kDa
LC3-II vs. Tubulin
0.8
0.6
0.4
0.2
0.0
***
###
***
METH - +
C
siCt
siCES1
METH - + - +
LC3-I
LC3-II
18 kDa
16 kDa
α-tubulin
50 kDa
LC3-II vs. Tubulin
2.5
2.0
1.5
1.0
0.5
0.0
*
##
**
METH - +

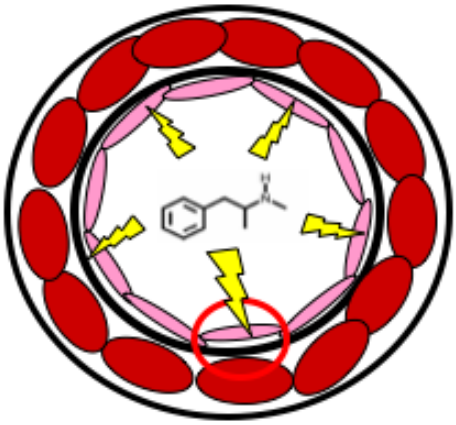

METH Exposure
(IV, inhaled, oral)

CYP2D6

P-OHMA

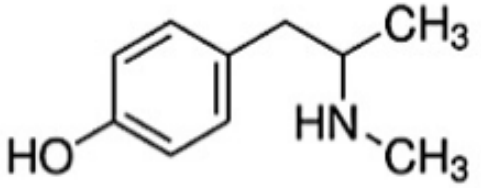

Toxic metabolites
(e.g. esters)

CES1

Reduced CES1
Expression/activity

ROS

Appropriate
Autophagic Flux

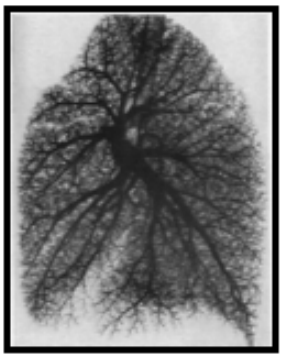

PMVEC
Recovery

ROS

Inappropriate
Autophagic Flux

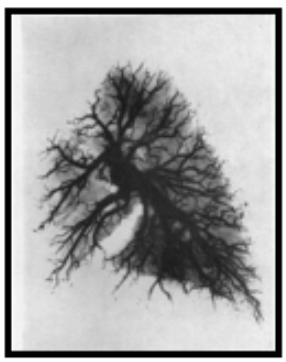

PMVEC
Apoptosis

	METH-PAH cohort (N=18)
Age - yrs	**47.8±6.7**
Gender - M,F (%)	**7, 11 (62%)**
BMI - kg/m2	**29.5±3.8**
NYHA - n (%)	
I	**3 (16.7)**
II	**6 (33.3)**
III	**8 (44.4)**
IV	**1 (5.6)**
6MWD - m	**486±145**
Therapies - n (%)	
Prostacyclin	**12 (66.7)**
ERA	**12 (66.7)**
PDE-I	**15 (83.3)**
CCB	**2 (11.1)**
Hemodynamics	
mRA - mmHg	**10.3±6.3**
mPAP - mmHg	**51.8±15.8**
PCWP - mmHg	**11.4±4.5**
CO - L/min	**4.2±1.0**
PVR - WU	**10.7±6.0**

Values represent Mean±SD, PAH = pulmonary arterial hypertension, BMI = Body mass index, iPAH=idiopathic PAH, NYHA = new york heart association symptom class, 6MWD = six minute walk distance, NT-pro BNP = N-terminal pro B-type naturietic peptide, ERA = endothelin-1 receptor antagonist, PDE-I = phosphodiesterase inhibitor, CCB = calcium channel blocker, mRA = mean right atrial pressure, mPAP = mean pulmonary artery pressures, PCWP = pulmonary capillary wedge pressure, CO = cardiac output, PVR = pulmonary vascular resistance

CYP2D6 SNV	Predicted Allele Freq	Allele Frequency IPAH	Allele Frequency METH-PAH	Function	AA Switch	AA Position
rs5030867	0.05%	9%	0%	Missense	His⇒Pro	324
rs1058172	16.7%	63.6%	58.8%	Missense	Arg⇒His	365
rs16947	66%	95%	95%	Missense	Arg⇒Cys	296
rs1135840	64%	64%	82.3%	Missense	Ser⇒Thr	486
rs1135828	0.23%	9.1	0%	Missense	Met⇒Lys	279
rs28371704	17%	9%	26.3%	Missense	His⇒Arg	94
rs28371703	16.3%	9%	10.5%	Missense	Leu⇒Met	91

CES1 SNV	Predicted Allele Freq	Allele Frequency PAH	Allele Frequency METH-PAH	Function	AA Switch	AA Position
rs115629050	3.1%	0%	94.4%	Missense	Ala ⇒ Ser	270
rs3826193	35.6%	64%	94.4%	Missense	Ile ⇒ Val	50
rs3826192	32.6%	64%	94.4%	Missense	Val ⇒ Ile	39
rs62028647	42%	72.7%	0%	Missense	Ser ⇒ Leu	82
rs2307240	5%	9%	0%	Missense	Ser ⇒ Asn	75

Gene	SNV	Allele Freq	Function	AA Switch	AA Position	Affected Carriers
BMPR2	rs2228545	3.92%	Missense	Ser ⇒Asn	775	2
BMP3	rs6831040	1.0%	Missense	Leu⇒Phe	205	18
BMP1	rs11996036	5.7%	Missense	Val⇒Ile	719	1
BMPR1A	rs3182217	35.6%	Missense	Pro ⇒ Thr	657	7
BMP4	rs17563	55.6%	Missense	Val ⇒ Ala	152	16
SMAD9	rs111748421	0.23%	Missense	Leu ⇒ Pro	22	1
SMAD3	rs35874463	5.2%	Missense	Ile ⇒ Val	170	1
SMAD7	rs3764482	19.15%	Missense	Ser ⇒ Phe	28	4